Chemistry–A European Journal
Research Article
doi.org/10.1002/chem.202300035
Chemistry Europe
European Chemical Societies Publishing
www.chemeurj.org

Synthesis of Sterically Encumbered Alkaline-Earth Metal Amides Applying the In Situ Grignard Reagent Formation

Simon Sengupta,[a] Philipp Schüler,[a] Phil Liebing,[a] and Matthias Westerhausen*[a]

Abstract: Magnesium and calcium are too inert to deprotonate amines directly. For the synthesis of bulky amides alternative strategies are required and in the past, *N*-bound trialkylsilyl groups have been used to ease metalation reactions. The in situ *Grignard* reagent formation in stirred suspensions of magnesium or calcium with hydryl halide and imine in THF allows the synthesis of a plethora of amides with bulky silyl-free substituents. Ball milling protocols partially favor competitive side reactions such as aza-pinacol coupling reactions. Calcium is the advantageous choice for the in situ *Grignard* reagent formation and subsequent addition onto the imines yielding bulky calcium bis(amides) whereas the stronger reducing heavier alkaline-earth metals strontium and barium are less selective and hence, the aza-pinacol coupling reaction becomes competitive. Exemplary, the solid-state molecular structures of $[(Et_2O)Mg(N(Ph)(CHPh_2)_2]$ and $[(Et_2O)_2Ca(N(Ph)(CHPh_2)_2]$ have been determined.

Introduction

The amides of the environmentally benign alkaline-earth metals magnesium and calcium are widely used reagents in stoichiometric reactions (metalation, transamination and salt-metathesis reactions) and catalytic conversions (hydrofunctionalization of unsaturated compounds) and nowadays also as electrolytes in batteries.[1] Especially magnesium amides attract tremendous attention because the reactivity of these reagents can easily be tuned and adapted to the substrate. Homoleptic magnesium bis(amides) $Mg(NR_2)_2$ and heteroleptic *Hauser* bases, i.e. R_2N–Mg-X, are important metalation reagents in organic and organometallic chemistry.[2] The metalation force can be enhanced via formation of their heterobimetallic derivatives.[3] Thus, lithium halide adducts, i.e. R_2N–Mg-X·LiX (turbo-*Hauser* bases),[4] and the inverse crowns, i.e. $ANR_2/Mg(NR_2)_2$ mixtures of alkali metal A and magnesium amides (*Mulvey* reagents),[5] are representative examples of highly reactive amide bases. Direct metalation of amines with magnesium and calcium is not viable due to the inertness of these metals even after activation (e.g. as powders or amalgams). To circumvent multiple-step procedures (preparation of *Grignard* reagent solution, magnesiation of amine, addition of stoichiometric amounts of anhydrous MgX_2 and LiX) the in situ *Grignard* Metalation Method (iGMM,[6] Scheme 1) proves to be highly advantageous. Here, bromoethane is added to an ethereal suspension of Mg turnings and amine yielding *Hauser* bases.

Calcium amides are far less common metalation reagents mainly due to challenging access paths.[7] Early attempts to synthesize $Ca(NR_2)_2$ via metalation of organic amines with calcium in liquid ammonia yielded insoluble and poorly characterized powders.[8] Homogeneous reaction conditions in stoichiometric and catalytic reactions could be ensured by applying highly soluble $Ca(hmds)_2$ [hmds = bis(trimethylsilyl)amide],[7,9] but the preparation posed severe drawbacks such as preparative challenges, extensive substrate preparation or use of toxic heavy-metal containing substrates. To avoid these disadvantages the iGMM was applied[10] allowing the straightforward multigram synthesis of $[(thf)_2Ca(hmds)_2]$ with high yields within a few hours. In contrast to the preparation of Mg-based *Hauser* bases, the transfer to the Ca-based iGMM is not generally feasible for a broad spectrum of amines due to competing reactions after formation of EtCaBr including iGMM, *Wurtz*-type coupling, alkylation of amine, and ether cleavage reactions (Scheme 2). In addition, strongly *Lewis* basic THF must be used for high conversion rates because thf adducts are soluble avoiding precipitation onto the calcium particle surface.

In contrast to the arylcalcium bromides and iodides, the alkylcalcium reagents are much more aggressive and enhance

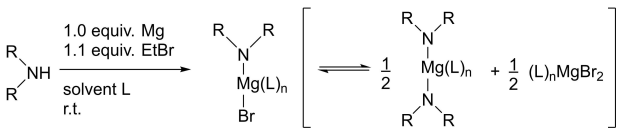

Scheme 1. In-situ *Grignard* Metalation Method (iGMM) for the straightforward synthesis of heteroleptic *Hauser* bases that may show a *Schlenk*-type equilibrium yielding the homoleptic compounds $[(L)_nMg(NR_2)_2]$ and magnesium bromide.

[a] *S. Sengupta, Dr. P. Schüler, Dr. P. Liebing, Prof. Dr. M. Westerhausen*
Institute of Inorganic and Analytical Chemistry
Friedrich Schiller University Jena
Humboldtstraße 8, 07743 Jena (Germany)
E-mail: m.we@uni-jena.de
Homepage: www.westerhausen.uni-jena.de

Supporting information for this article is available on the WWW under https://doi.org/10.1002/chem.202300035

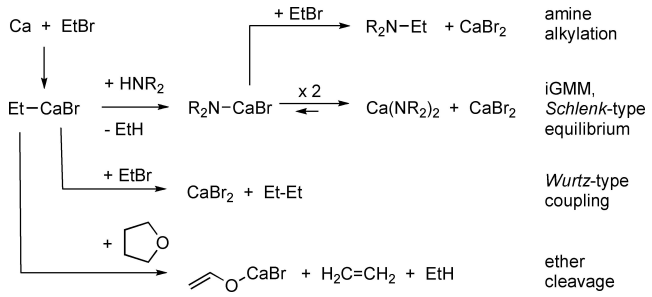

Scheme 2. Competing reactions and outcome of the calcium-based iGMM (from top to bottom: alkylation of amine, amidocalcium bromide formation and *Schlenk*-type equilibrium, *Wurtz*-type coupling reaction, ether degradation; solvation of the calcium atom by ether molecules is omitted for clarity reasons).

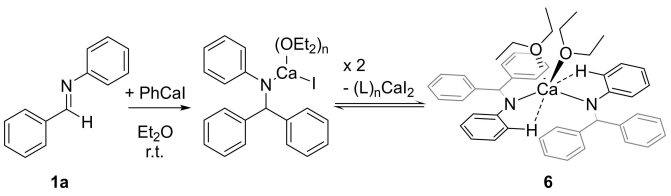

Scheme 3. Synthesis and *Schlenk*-type equilibrium of heteroleptic calcium-based *Hauser* base and formation of homoleptic $[(Et_2O)_2Ca\{N(Ph)CHPh_2\}_2]$ and calcium iodide.

the tendency to side reactions. Ether cleavage occurs within a time frame of a few hours, but *Wurtz*-type coupling reactions can become the major reaction path.[11]

The key step of calcium-based *Grignard* reagent formation is the reduction of aryl- or alkylhalide by calcium. First attempts date back to 1905 when *Beckmann* reacted Ca granules with organic halides,[12] but later investigations by *Gilman* and coworkers mistrusted these studies.[13] Severe side reactions also aggravated isolation of pure products.[14] Trapping experiments by the *Kawabata* group supported intermediate formation of calcium-type *Grignard* reagents from organic halides and calcium turnings.[15] Till this day, a straightforward strategy for the synthesis of alkylcalcium via direct synthesis is still lacking despite the finding that methylcalcium iodide and dimethylcalcium are manageable and stable compounds.[16] The major reason is the competitive *Wurtz*-type coupling reaction which becomes the dominating pathway for aliphatic hydrylcalcium halides.

Results and Discussion

The straightforward synthesis of *Hauser* bases via the iGMM encouraged us to broaden the application of in situ *Grignard* reagent formation not only for metalation but also for addition reactions. The reaction of PhCaI with *N*-benzylidene-aniline (**1 a**) and subsequent hydrolysis yielded quantitatively *N*-benzhydrylaniline (**4 a**) whereas neither PhMgX nor PhMgX·LiX reacted with this imine. The addition of PhCaI onto *E*-Ph-HC=NPh in diethyl ether and subsequent *Schlenk*-type ligand redistribution gave orange $[(Et_2O)_2Ca\{N(Ph)CHPh_2\}_2]$ (**6**, Scheme 3).

Simplification of this protocol by using the in situ *Grignard* reagent formation protocol avoided isolation and purification of calcium-based *Grignard* reagents as well as large concentrations of calcium-based *Grignard* reagents. In this procedure, phenyl iodide was added at room temperature to a suspension of calcium granules and imine in THF applying an excess of calcium and hydryl halide. Within the initial ten minutes, the color of the reaction mixture turned from colorless over yellow-orange to red and finally red-brown. Hydrolysis after stirring overnight gave a yield of 82% of *N*-benzhydrylaniline (**4 a**). Besides this major reaction, calcium could directly reduce the imine yielding small amounts of 1,2-dianilino-1,2-diphenylethane (**3 a**, one-electron transfer and C–C coupling, aza-pinacol coupling, 6%) and benzylaniline (**2 a**, two-electron reduction, 2%). Calcium complexes via a 2-electron reduction of diphenylmethylene-aniline and benzhydrylanilido calcium complexes have been recognized earlier.[17] These pathways are depicted in Scheme 4 whereas *Wurtz*-type coupling (reaction of RCaX with RX to R–R and CaX_2) and ether degradation reactions (formation of RH and Ca alcoholates) are neglected in this Scheme. Magnesium was significantly less reactive and under very similar reaction conditions, a conversion of only 10% was observed.

To elucidate optimized reaction conditions for this in situ *Grignard* Addition Method (iGAM), different ethereal solvents and aryl as well as alkyl iodides were tested. In THF high yields were achieved whereas in less *Lewis* basic diethyl ether and

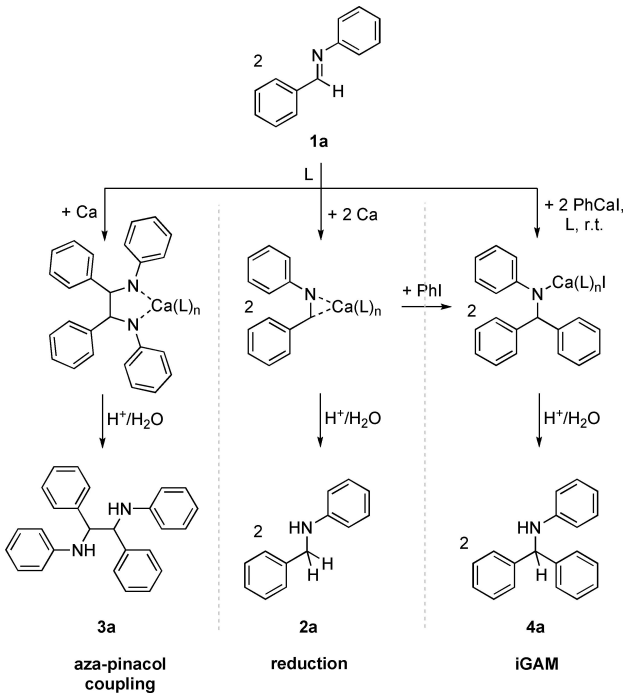

Scheme 4. Reaction of benzylidene-aniline with phenylcalcium iodide and calcium metal in ethereal solvents L (such as THF, Et_2O and others, see text) leading to iGAM, reduction and aza-pinacol coupling.

cyclopentyl-methylether or sterically more demanding 2-methyltetrahydrofuran roughly equal amounts of addition and aza-pinacol coupling products were formed. Nevertheless, the complexes **5** and **6** were crystallized from these reaction mixtures as shown in Scheme 5. In contrast, 1,4-dioxane and methyl-(*tert*-butyl)ether were inapplicable and no conversion was observed. In all solvents, production of benzylaniline occurred not or only in trace amounts.

Variation of the aryl iodide allowed the synthesis of differently substituted benzhydrylanilines (at the top of Scheme 6). Iodobenzene and 1-iodonaphthalene gave high conversion rates and the major products were the addition products. The influence of *para*-bound chloro and *meta*-positioned methyl and methoxy groups is rather small. In contrast, *ortho*-positioned methyl and *tert*-butyl substituents favor the formation of the aza-pinacol coupling products with yields of 76% and 60%, respectively, because steric hindrance significantly decelerated the addition reaction. In addition, the slower conversion promoted ether degradation via deprotonation of THF, and subsequent addition onto benzylidene-aniline yielded minor amounts of *N*-[phenyl(tetrahydrofuran-2-yl)methyl]aniline (Scheme 7). Replacement of the aryl iodides by homologous bromides led to preferred aza-pinacol coupling reactions.

Repetition of the iGAM in a ball mill led to an improved yield of 49% for the magnesium-based protocol, namely the reaction of magnesium and iodobenzene with *N*-benzylidene-aniline in the presence of a very small amount of THF to benzhydrylanilido magnesium iodide (Table 1). For calcium and strontium, yields of 61% and 71% in the same order of magnitude, respectively, were obtained. For more reactive barium, the aza-pinacol coupling reaction was favored (37%), whereas the formation of benzhydrylaniline was disadvantaged (40%). Again, change of the halide and use of bromobenzene led to enhanced amounts of the aza-pinacol coupling products at the expense of the addition products. In the ball milling procedure, several alkyl iodides were applied. Ethyl, *n*-butyl and *n*-octyl iodide led to preferred formation of the addition products as depicted in Scheme 6. A lower yield of 51% was obtained for isopropyl iodide, assumedly due to steric hindrance.

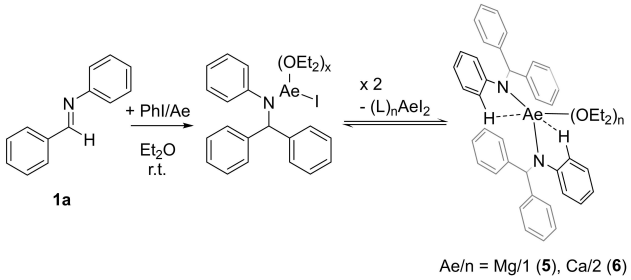

Scheme 5. Synthesis and of homoleptic magnesium and calcium-compounds $[(Et_2O)_nAe\{N(Ph)CHPh_2\}_2]$ (Ae/n = Mg/1 (**5**) and Ca/2 (**6**)).

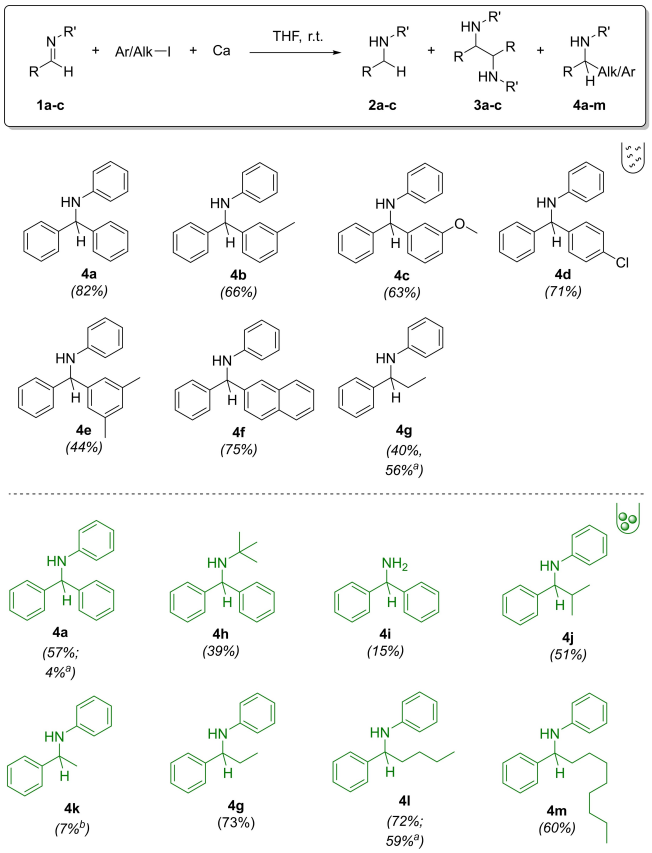

Scheme 6. Substrate scope of the addition of aryl and alkyl halides onto imines using the in situ *Grignard* Addition Method (iGAM) in a 0.5 M THF solution at room temperature with a molar 1.0:1.5:1.5 ratio of imine, Ca and RX (top, black lettering) and in a ball milling procedure (green lettering)

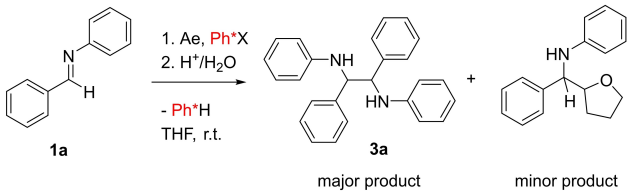

Scheme 7. Application of bulky aryl halides (Ph* = Mes, C_6H_2-2,4,6-tBu_3) leads to competing aza-pinacol coupling (major product) and ether cleavage via deprotonation of THF with subsequent addition onto benzylidene-aniline yielding minor amounts of *N*-(phenyl(tetrahydrofuran-2-yl)methyl)aniline.

Table 1. Product distribution using different alkaline-earth metals in the addition of aryl halides onto imines using the iGAM. In addition, various preparative procedures were compared.

Entry	Metal	Yield [%] in solution[a]			ball mill[b]			ball mill w/o PhI[b]		
		2a	**3a**	**4a**	**2a**	**3a**	**4a**	**2a**	**3a**	**4a**
1	Mg	1	4	10	2	2	49	4	56	-
2	Ca	2	6	82	2	3	61	2	27	-
3	Sr	3	10	75	4	8	71	3	67	-
4	Ba	2	78	8	4	37	40	2	83	-

[a] Yields are determined after 17 h reaction time by proton NMR of a quenched aliquot. [b] Yields are determined after 1 h reaction time by proton NMR of an quenched aliquot.

In Table 1 the iGAM in THF solution and according to a ball milling protocol are compared for the alkaline-earth metals. In addition, absence of iodobenzene led mainly to the aza-pinacol coupling product. For calcium the addition product was the preferred product in solution with a very good yield of 82%. Increasing reactivity of the alkaline-earth metals eased electron transfer onto the imine increasing the aza-pinacol coupling products. In the absence of iodobenzene, the aza-pinacol coupling reaction was accelerated for the heavier alkaline-earth metals. This finding is in agreement with the observation that the addition product and hence, the intermediate formation of PhCaI, is preferred for calcium, whereas barium was the most effective reducing reagent for the imine substrate.

Surprisingly, methyl iodide reacted differently in the ball milling procedure than the other aryl and alkyl halides. In a very similar protocol, only 7% of the benzylidene-aniline was converted to *N*-(1-phenylethyl)aniline and the major product was *N*-(1-phenylethyl)-*N*-methylaniline. The initial reaction step is the formation of *N*-(1-phenylethyl)anilido calcium iodide which reacted with another equivalent of methyl iodide yielding *N*-(1-phenylethyl)-*N*-methylaniline and calcium iodide (Scheme 8). If ethyl iodide was applied in this protocol, the iGAM (73%) and *N*-alkylation reaction (8%) were competing processes.

Alkaline-earth metal complexes with low-coordinate metals commonly exhibit high reactivity due to accessibility of the highly Lewis acidic metal ions toward substrate molecules.[18] The solid-state molecular structures and atom labeling schemes of $[(Et_2O)Mg\{N(Ph)CHPh_2\}_2]$ (**5**) and $[(Et_2O)_2Ca\{N(Ph)CHPh_2\}_2]$ (**6**) are depicted in Figures 1 and 2.[19] Intramolecular repulsion between the bulky benzhydryl substituents leads to relatively large N1-Mg1-N1′ and Mg1-N1-C7 bond angles. The magnesium atoms are nearly in a T-shaped coordination sphere.

In $[(Et_2O)_2Ca\{N(Ph)CHPh_2\}_2]$ (**6**) the metal atom is in a distorted tetrahedral coordination sphere. Agostic interactions (broken lines) lead to an asymmetric binding of the phenyl groups (N1-C1-C2 118.0(2)°, N1-C1-C6 126.5(2)°) as has also been observed in the magnesium congener. In comparison to $[(thf)_2Ca\{N(SiMe_3)_2\}_2]$ (Ca–N 229.4(3) and 230.9(3) pm, Ca–O 236.9(3) and 238.5(3) pm), larger Ca1-N1 and Ca1-O1 distances are observed because the negative charge is delocalized within the anilido substructure and Et_2O is a weaker *Lewis* base than THF. In both alkaline-earth metal complexes the bulky benzhydryl substituents stabilize small coordination numbers of the metal centers.

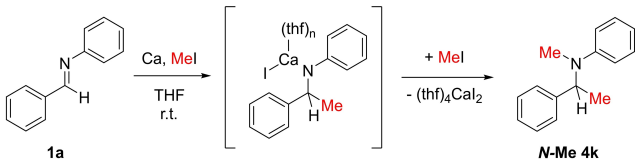

Scheme 8. Amine alkylation using methyl iodide in the iGAM of benzylidene-aniline in THF at room temperature.

Conclusions

The iGAM offers a straightforward method for the synthesis of secondary amides that can be very bulky being able to stabilize complexes with low-coordinate alkaline-earth metals. The solvent has a strong influence on reaction pathway and product distribution (Scheme 9). THF is the preferred ethereal solvent for the iGAM in solution because it effectively coordinates the metal ions and ensures solubility of the intermediately formed

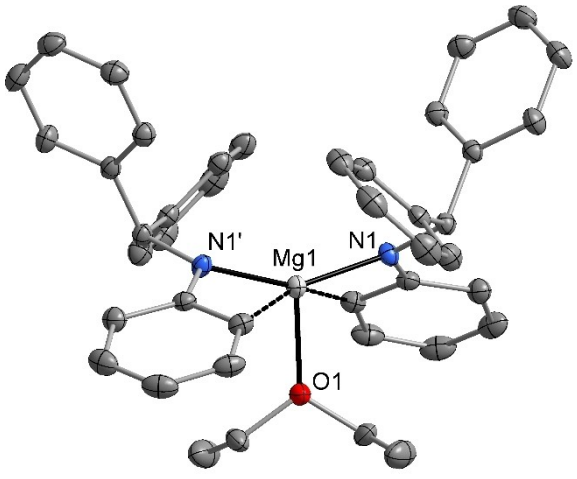

Figure 1. Molecular structure of $[(Et_2O)Mg\{N(Ph)CHPh_2\}_2]$ (**5**) in the crystal (left). Displacement ellipsoids drawn at the 50% probability level, H atoms omitted for clarity. Atoms Mg1 and O1 are situated on a crystallographic two-fold rotational axis. Symmetry code to generate equivalent atoms: '1-x, y, 0.5-z. Selected bond lengths (pm): Mg1-O1 201.08(13), Mg1-N1 197.14(9), N1-C1 137.99(13), N1-C7 145.64(13); angles (deg.): N1-Mg1-N1′ 150.58(6), N1-Mg1-O1 104.71(3), Mg1-N1-C1 116.94(7), Mg1-N1-C7 123.76(7), C1-N1-C7 116.54(9).

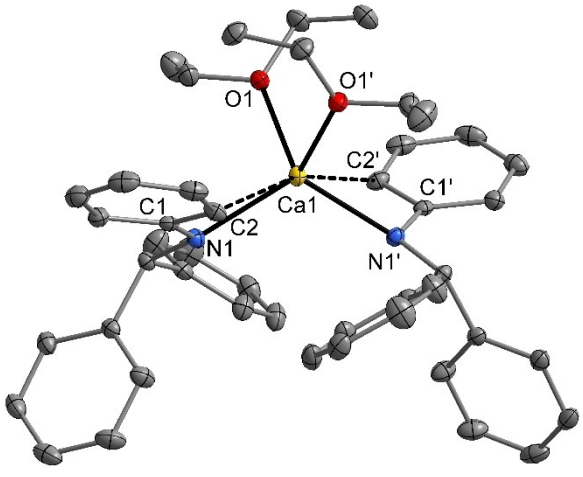

Figure 2. Molecular structure and atom labelling scheme of $[(Et_2O)_2Ca\{N(Ph)CHPh_2\}_2]$ (**6**) in the crystal. The ellipsoids represent a probability of 40%, H atoms are omitted for the sake of clarity. Selected bond lengths (pm): Ca1-O1 240.2(2), Ca1-N1 233.7(2), Ca1-C1 306.2(2), Ca1-C2 310.9(2), N1-C1 137.2(3), N1-C7 145.6(3); angles (deg.): O1-Ca1-O1′ 92.02(9), N1-Ca1-N1′ 117.26(9), N1-Ca1-O1 102.20(6), N1-Ca1-O1′ 120.79(6), Ca1-N1-C1 108.5(1), Ca1-N1-C7 129.7(1), C1-N1-C7 115.5(2).

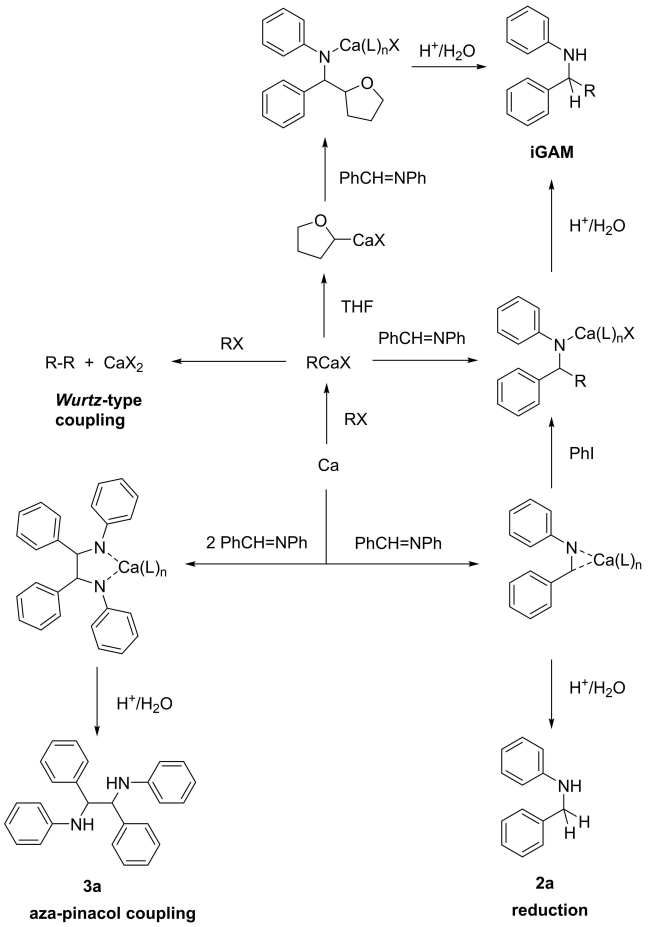

Scheme 9. Synthesis and *Schlenk*-type equilibrium of heteroleptic calcium-based *Hauser* base and formation of homoleptic $[(Et_2O)_2Ca\{N(Ph)CHPh_2\}_2]$ (**6**) and calcium iodide.

calcium complexes such as *Grignard*-type RCaX, amidocalcium halides and calcium bis(amides). In the ball milling process, the yields are lower. Unique exceptions are small alkyl iodides which react during ball milling mainly to *N*-alkylated anilines. In ethereal solution, the amido magnesium halides and amido calcium halides show *Schlenk*-type ligand redistribution reactions yielding homoleptic alkaline-earth metal bis(amides). The bulky benzhydrylanilides stabilize small coordination numbers of three and four for magnesium and calcium, however, short contacts to aryl groups shield the metal atoms additionally. These procedures allow the synthesis of a plethora of amides without the necessity of supporting trialkylsilyl substituents for enhanced reactivity of the amine substrates and solubility of the alkaline-earth metal amides.

This reaction allows to compare the iGAM in solution and during the ball milling process. In THF solution, the reaction periods are much longer and therefore, the tendency to form side products increases. In addition, the ball milling protocol requires significantly less THF solvent but after the reaction time, the products are washed out by an appropriate solvent. The allurement of these methods, however, is a different product distribution and hence, realization of the iGAM in solution or in a ball mill can yield different major products and complement one another.

Experimental Section

General: All manipulations were carried out under an inert nitrogen atmosphere using standard *Schlenk* techniques, if not otherwise noted. The solvents were dried over KOH and subsequently distilled over sodium/benzophenone under a nitrogen atmosphere prior to use. All substrates were purchased from Alfa Aesar, abcr, Sigma Aldrich or TCI and used without further purification. *N-Tert*-butyl-1-phenylmethaneimine[20] and 1-phenyl-*N*-(trimethylsilyl)-methaneimine[21] were synthesized as described in the literature. Mechanochemical synthesis was performed using a Retsch MM 301 ball-mill with 5 mL stainless steel grinding jars containing eight 3 mm stainless steel balls. The yields given are not optimized. Purity of the compounds was verified by NMR spectroscopy. Deuterated solvents were dried over sodium, distilled, degassed, and stored under nitrogen over sodium. ^{1}H and ^{13}C{^{1}H} NMR spectra were recorded on Bruker Fourier 300 and Bruker Avance III 400 (BBO, BBFO probes) spectrometers. Chemical shifts are reported in parts per million relatively to $SiMe_4$ as an external standard referenced to the solvents residual proton signal using the *xiref* AU program for ^{13}C NMR spectra. DOSY NMR spectra were measured using the convection compensated *dstebpgp3 s* standard pulse sequence. Molar masses in solution were calculated using the *Stalke*-ECC-DOSY method.[22] ASAP-HSQC-spectra and ASAP-HSQC-DEPT-spectra were recorded using the published pulse sequences.[23] NOAH experiments were performed using the GENESIS tool based on the published pulse programs.[24] The elemental analysis gave no reliable results due to loss of ligated ethers during handling and combustion.

General procedure of iGAM

In solution: Alkaline-earth metal (1.0 equiv.) and imine (1.5 equiv.) were suspended in an ethereal solvent (0.25–0.5 M). Alkyl/aryl halides (1.5 equiv.) were added at room temperature and the reaction mixture was stirred overnight at room temperature.

Mechanochemical (Ball mill): Alkaline-earth metal (~1.0 mmol, 1.0 equiv.) and imine (~1.5 mmol, 1.5 equiv.) were suspended in an ethereal solvent (0.2 mL, ~5 M) under argon atmosphere. Alkyl/aryl halides (1.5 equiv.) were added at room temperature and the reaction mixture was shaken for 1 h at room temperature.

Work-Up: The reaction mixture was quenched with a saturated ammonium chloride solution and the organic layer was separated. The solvents were removed under reduced pressure and the oily residue was purified by column chromatography (PE/EtOAc, 9:1).

General procedure for aza-pinacol-coupling

Mechanochemical (Ball mill): Alkaline-earth metal (~1.0 mmol, 1.0 equiv.) and imine (~1.5 mmol, 1.5 equiv.) were suspended in an ethereal solvent (0.2 mL, ~5 M) under argon atmosphere. The reaction mixture was shaken for 1 h at room temperature.

The reaction mixture was quenched with a saturated ammonium chloride solution and the organic layer was separated. The solvents were removed under reduced pressure and the oily residue was purified by column chromatography (PE/EtOAc, 9:1).

Synthesis of $[(C_{19}H_{16}N)_2Mg(Et_2O)]$ (5) via iGAM: *N*,1-Diphenylmethaneimine (608.5 mg, 3.4 mmol, 1.0 equiv.) and magnesium turnings (120.3 mg, 4.9 mmol, 1.5 equiv.) were suspended in Et_2O (7.0 mL). Ph–I (0.6 mL, 5.0 mmol, 1.5 equiv.) was added at room temperature and the reaction mixture was stirred overnight at room temperature. Et_2O was removed under reduced pressure and the oily residue was redissolved in toluene (3.0 mL). The deep red solution was stored for 5 days at ambient temperature, yielding the amide as yellow crystals. Yield: 242.0 mg, 0.4 mmol, 23 %. Analytical data for $([(C_{19}H_{16}N)_2Mg(Et_2O)]$: ^{1}H NMR: (300 MHz, $[D_8]$toluene, 297 K): δ = 7.40–7.32 (m, 8H), 7.23–7.00 (m, 14H), 6.95 (t, 6H), 6.51 (t, 2H), 5.48 (s, 2H), 3.43–3.11 (m, 4H, Et_2O), 1.04–0.72 (m, 6H, Et_2O). ^{13}C NMR: (75 MHz, $[D_8]$toluene, 297 K): 159.5, 129.3, 128.8, 128.6, 127.9, 127.1, 114.9, 65.7, 13.9.

Synthesis of $[(C_{19}H_{16}N)_2Ca(Et_2O)_2]$ (6) via addition of *Grignard* reagent: *N*,1-Diphenylmethaneimine (488.8 mg, 2.7 mmol, 1.0 equiv.) was dissolved in Et_2O (20.0 mL). PhCaI (3.6 mL, 0.75 M, 1.0 equiv.) in Et_2O was added in one portion and the reaction mixture was stirred for 1 h at room temperature. The deep red solution was stored for 3 days at ambient temperature. The dark red crystalline precipitate was collected and dried under reduced pressure. Yield: 720.0 mg, 1.02 mmol, 75 %. Analytical data for $([(C_{19}H_{16}N)_2Ca(Et_2O)_2]$: ^{1}H NMR: (400 MHz, $[D_8]$toluene, 297 K): δ = 7.39–7.27 (m, 10H), 7.08–6.90 (m, 20H), 5.42 (s, 2H), 3.29 (q, 8H, Et_2O), 1.13 (t, 12H, Et_2O), ^{13}C NMR: (101 MHz, $[D_8]$toluene, 297 K): δ = 157.1, 146.3 131.1, 129.5, 128.9, 128.8, 127.5, 127.1, 114.3, 66.6, 65.5, 15.1.

X-ray diffraction experiments at single crystals:[19] The single-crystal X-ray intensity data for the reported compounds were collected on a Bruker-Nonius Kappa-CCD diffractometer equipped with a Mo–Kα IμS microfocus source and an Apex2 CCD detector, at T = 120(2) K. The crystal structures were solved with SHELXT-2018/3[25] and refined by full matrix least-squares methods on F^2 with SHELXL-2018/3,[26] using the Olex 1.2 environment.[27] Multi-scan absorption correction was applied to the intensity data.[28]

Supporting Information

Experimental details, NMR spectra, tables with screening experiments, crystallographic and refinement data of crystal structures, ball-and-stick drawings of **5** and **6**.

Acknowledgements

We acknowledge the valuable support of the NMR and MS service platforms (www.nmr.uni-jena.de; www.ms.uni-jena.de) of the Faculty of Chemistry and Earth Sciences of the Friedrich Schiller University Jena, Germany. Open Access funding enabled and organized by Projekt DEAL.

Conflict of Interest

The authors declare no conflict of interest.

Data Availability Statement

The data that support the findings of this study are available in the supplementary material of this article.

Keywords: alkaline-earth metals · Barbier reaction · bulky amides · Grignard reaction · mechanochemistry

[1] a) S. Dongmo, S. Zaubitzer, P. Schüler, S. Krieck, L. Jörissen, M. Wohlfahrt-Mehrens, M. Westerhausen, M. Marinaro, *ChemSusChem* **2020**, *13*, 3530–3538; b) S. Zaubitzer, S. Dongmo, P. Schüler, S. Krieck, F. Fiesinger, D. Gaissmaier, M. van den Borg, T. Jacob, M. Westerhausen, M. Wohlfahrt-Mehrens, M. Marinaro, *Energy Technol.* **2022**, *10*, 2200440; c) P. Schüler, S. Sengupta, S. Zaubitzer, F. Fiesinger, S. Dongmo, H. Görls, M. Wohlfahrt-Mehrens, M. van den Borg, D. Gaissmaier, S. Krieck, M. Marinaro, T. Jacob, M. Westerhausen, *Eur. J. Inorg. Chem.* **2022**, e202200149.
[2] a) K. W. Henderson, W. J. Kerr, *Chem. Eur. J.* **2001**, *7*, 3430–3437; b) J.-C. Plaquevent, T. Perrard, D. Cahard, *Chem. Eur. J.* **2002**, *8*, 3300–3307; c) M. Westerhausen, *Dalton Trans.* **2006**, 4755–4768; d) R. E. Mulvey, *Acc. Chem. Res.* **2009**, *42*, 743–755; e) A. Harrison-Marchand, F. Mongin, *Chem. Rev.* **2013**, *113*, 7470–7562.
[3] a) R. E. Mulvey, F. Mongin, M. Uchiyama, Y. Kondo, *Angew. Chem. Int. Ed.* **2007**, *46*, 3802–3824; *Angew. Chem.* **2007**, *119*, 3876–3899; b) A. J. Martínez-Martínez, C. T. O'Hara, *Adv. Organomet. Chem.* **2016**, *65*, 1–46; c) S. D. Robertson, M. Uzelac, R. E. Mulvey, *Chem. Rev.* **2019**, *119*, 8332–8405.
[4] a) P. Knochel, T. Thaler, C. Diene, *Isr. J. Chem.* **2010**, *50*, 547–557; b) B. Haag, M. Mosrin, H. Ila, V. Malakhov, P. Knochel, *Angew. Chem. Int. Ed.* **2011**, *50*, 9794–9824; *Angew. Chem.* **2011**, *123*, 9968–9999; c) A. D. Benischke, M. Ellwart, M. R. Becker, P. Knochel, *Synthesis* **2016**, *48*, 1101–1107.
[5] a) R. E. Mulvey, *Chem. Commun.* **2001**, 1049–1056; b) R. E. Mulvey, *Organometallics* **2006**, *25*, 1060–1075; c) A. J. Martínez-Martínez, A. R. Kennedy, R. E. Mulvey, C. T. O'Hara, *Science* **2014**, *346* (6211), 834–837; d) A. J. Martínez-Martínez, D. R. Armstrong, B. Conway, B. J. Fleming, J. Klett, A. R. Kennedy, R. E. Mulvey, S. D. Robertson, C. T. O'Hara, *Chem. Sci.* **2014**, *5*, 771–781.
[6] S. Sengupta, P. Schüler, H. Görls, P. Liebing, S. Krieck, M. Westerhausen, *Chem. Eur. J.* **2022**, *28*, e202201359.
[7] M. Westerhausen, *Trends in Organometallic Chemistry* **1997**, *2*, 89–105; M. Westerhausen, *Coord. Chem. Rev.* **1998**, *176*, 157–210; A. Torvisco, A. Y. O'Brien, K. Ruhlandt-Senge, *Coord. Chem. Rev.* **2011**, *255*, 1268–1292.
[8] A. R. Utke, R. T. Sanderson, *J. Org. Chem.* **1964**, *29*, 1261–1264.
[9] M. P. Coles, *Coord. Chem. Rev.* **2015**, *297–298*, 2–23.
[10] a) S. Krieck, P. Schüler, J. M. Peschel, M. Westerhausen, *Synthesis* **2019**, *51*, 1115–1122; b) P. Schüler, S Sengupta, A. Koch, H. Görls, S. Krieck, M. Westerhausen, *Chem. Eur. J.* **2022**, *28*, e202201897.
[11] A. Koch, Q. Dufrois, M. Wirgenings, H. Görls, S. Krieck, M. Etienne, G. Pohnert, M. Westerhausen, *Chem. Eur. J.* **2018**, *24*, 16840–16850.
[12] E. Beckmann, *Ber. Dtsch. Chem. Ges.* **1905**, *38*, 904–906.
[13] H. Gilman, F. Schulze, *J. Am. Chem. Soc.* **1926**, *48*, 2463–2467.
[14] D. Bryce-Smith, A. C. Skinner, *J. Chem. Soc.* **1963**, 577–585.
[15] a) N. Kawabata, A. Matsumura, S. Yamashita, *Tetrahedron* **1973**, *29*, 1069–1071; b) N. Kawabata, A. Matsumura, S. Yamashita, *J. Org. Chem.* **1973**, *38*, 4268–4270.
[16] a) B. M. Wolf, C. Stuhl, C. Maichle-Mössmer, R. Anwander, *J. Am. Chem. Soc.* **2018**, *140*, 2373–2383; b) For a recent review on alkylcalcium compounds see: D. O. Khristolyubov, D. M. Lynbov, A. A. Trifonov, *Russ. Chem. Rev.* **2021**, *90*, 529–565.
[17] F. Buch, S. Harder, *Organometallics* **2007**, *26*, 5132–5133.
[18] J. Martin, J. Eyselein, S. Grams, S. Harder, *ACS Catal.* **2020**, *10*, 7792–7799.
[19] Deposition Numbers 2226169 (for **5**) and −2226170 (for **6**) contains the supplementary crystallographic data for this paper. These data are provided free of charge by the joint Cambridge Crystallographic Data Centre and Fachinformationszentrum Karlsruhe Access Structures service.
[20] I. A. Cliffe, R. Crossley, R. G. Shepherd, *Synth.* **1985**, *12*, 1138–1140.
[21] A. Kuznetsov, A. V. Gulevich, D. J. Wink, V. Gevorgyan, *Angew. Chem. Int. Ed.* **2014**, *53*, 9021–9025; *Angew. Chem.* **2014**, *126*, 9167–9171.

[22] R. Neufeld, D. Stalke, *Chem. Sci.* **2015**, *6*, 3354–3364.
[23] a) D. Schulze-Sünnighausen, J. Becker, B. Luy, *J. Am. Chem. Soc.* **2014**, *136*, 4, 1242–1245; b) D. Schulze-Sünnighausen, J. Becker, M. R. M. Koos, B. Luy, *J. Magn. Reson.* **2017**, *281*, 151–161.
[24] a) J. R. J. Yong, Ē. Kupče, T. D. W. Claridge, *Anal. Chem.* **2022**, *94*, 2271–2278; b) Ē. Kupče, T. D. W. Claridge, *Angew. Chem. Int. Ed.* **2017**, *56*, 11779–11783; *Angew. Chem.* **2017**, *129*, 11941–11945; c) J. R. J. Yong, A. L. Hansen, Ē. Kupče, T. D. W. Claridge, *J. Magn. Reson.* **2021**, *329*, 107027.
[25] G. M. Sheldrick, *Acta Crystallogr. Sect. A* **2015**, *71*, 3–8.
[26] G. M. Sheldrick, *Acta Crystallogr. Sect. C* **2015**, *71*, 3–8.
[27] O. V. Dolomanov, L. J. Bourhis, R. J. Gildea, J. A. K. Howard, H. Puschmann, *J. Appl. Crystallogr.* **2009**, *42*, 339–341.
[28] Bruker AXS **2001**, *Apex4 and SADABS*, Bruker AXS Inc., Madison, Wisconsin, USA.

Manuscript received: January 5, 2023
Accepted manuscript online: February 3, 2023
Version of record online: March 15, 2023